



Imaging properties of a metamaterial superlens

Nicholas Fang and Xiang Zhang

Citation: [Applied Physics Letters](#) **82**, 161 (2003); doi: 10.1063/1.1536712

View online: <http://dx.doi.org/10.1063/1.1536712>

View Table of Contents: <http://scitation.aip.org/content/aip/journal/apl/82/2?ver=pdfcov>

Published by the [AIP Publishing](#)

Articles you may be interested in

[Study of nanospheres lithography technology with super-lens for fabricating nano holes](#)

J. Appl. Phys. **113**, 183102 (2013); 10.1063/1.4803845

[A smooth optical superlens](#)

Appl. Phys. Lett. **96**, 043102 (2010); 10.1063/1.3293448

[A superlens for the deep ultraviolet](#)

Appl. Phys. Lett. **95**, 121909 (2009); 10.1063/1.3226101

[Mechanisms of subdiffraction free-space imaging using a transmission-line metamaterial superlens: An experimental verification](#)

Appl. Phys. Lett. **92**, 131105 (2008); 10.1063/1.2904635

[Dynamic readout of subdiffraction-limited pit arrays with a silver superlens](#)

Appl. Phys. Lett. **87**, 211101 (2005); 10.1063/1.2132079



Imaging properties of a metamaterial superlens

Nicholas Fang and Xiang Zhang^{a)}

Department of Mechanical and Aerospace Engineering, University of California at Los Angeles, 420 Westwood Plaza, Los Angeles, California 90095

(Received 24 September 2002; accepted 18 November 2002)

The subwavelength imaging quality of a metamaterial superlens is studied numerically in the wave vector domain. Examples of image compression and magnification are given and resolution limits are discussed. A minimal resolution of $\lambda/6$ is obtained using a 36 nm silver film at 364 nm wavelength. Simulation also reveals that the power flux is no longer a good measure to determine the focal plane of superlens due to the elevated field strength at exit side of the metamaterial slab.

© 2003 American Institute of Physics. [DOI: 10.1063/1.1536712]

Metamaterials have opened an exciting gateway to create unprecedented physical properties and functionality unattainable from naturally existing materials. The “atoms” and “molecules” in metamaterials can be tailored in shape and size; the lattice constant and interatomic interaction can be artificially tuned, and “defects” can be designed and placed at desired locations. Pioneering work on strongly modulated photonic crystals¹ represent a giant step in engineered metamaterials. The recent discovery of left-handed metamaterials (LHM)^{2,3} with negative effective permittivity and permeability over a designed frequency band has attracted increasing interest in this field. A medium of this type was termed “left handed” originally by Veselago,⁴ because for an electromagnetic plane wave propagating inside the LHM, the direction of Poynting vector is opposite to the wave vector.

Veselago suggested that a rectangular slab of LHM could focus the electromagnetic radiation. More recently, Pendry⁵ predicted an intriguing property of such a LHM lens: Unlike conventional optical components, it will focus both the propagating spectra and the evanescent waves, thus capable of achieving diffraction-free imaging. From the quasistatic theory, Pendry further suggested that for near-field imaging, the permittivity and permeability of the metamaterial can be designed independently in accordance with different polarization. For example, a thin metal film with a negative value of permittivity is capable of imaging the transverse magnetic (TM) waves of the near-field object to the opposite side, with a resolution significantly below the diffraction limit.

However, Pendry’s quasistatic theory did not address the following questions: How does the loss and dielectric mismatch affect the imaging quality? Is it possible to achieve reduction or magnification with LHM? What is a good measure of the depth of focus in the superlens? In this letter, we present the full-wave numerical results by considering the retardation effect in attempt to answer these questions. Figure 1 depicts the two-dimensional (2D) imaging system in our study. For simplicity without loss of generality, we consider the imaging quality of two monochromatic line current sources transmitting through a metamaterial slab. The sources are embedded in medium 1 with uniform and isotropic permittivity ϵ_1 and permeability μ_1 , displaced by width

$2a$; the separation from the current sources to the slab is defined as the object distance, u . The electromagnetic field due to TM sources $\mathbf{J}(\mathbf{r}) = \hat{z}I\delta(\mathbf{r} - \mathbf{r}')$, located at $\mathbf{r}' = (x = \pm a, z = -u)$, travels through the metalens of thickness d with designed properties ϵ_M and μ_M , and reaches medium 2 where the images are formed at a distance v to the right-hand side of the lens.

The imaging capability associated with the LHM slabs is based on the effect of negative refraction.^{4–6} From paraxial-ray treatment in geometric optics, the refracted wave from the object will converge first inside the slab to produce a 2D image by transformation: $(x, y, -u) \rightarrow (x, y, |n_M/n_1|u)$; as the waves advance to reach the other surface of the slab, negative refraction occurs again to produce a second image in the half space of medium 2, located at $(x, y, (1 + |n_2/n_M|)d - |n_M/n_1|u)$. Therefore, paraxial analysis predicts that the image produced by a slab metalens is characterized by $v = |n_2/n_M|d - |n_M/n_1|u$.

The image quality of this model system can be quantified using the conventional optical transfer function (OTF), defined as the ratio of image field to object field, $H_{\text{img}}/H_{\text{obj}}$, with given lateral component of wave vector k_x . From Fresnel’s formula of the stratified medium, the optical transfer function of the metalens can now be written as

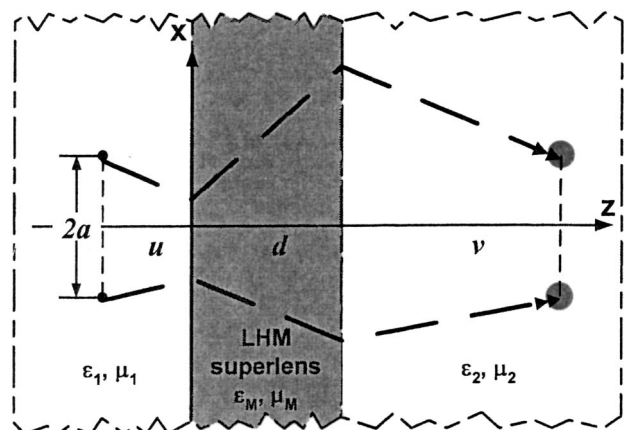


FIG. 1. The model of a LHM lens under the radiation of two line current sources.

^{a)}Electronic mail: xiang@seas.ucla.edu

$$\text{OTF}(k_x) = \frac{t_{1M} t_{M2} \exp(i\beta_M d) \exp(i\beta_1 u) \exp(i\beta_2 v)}{1 + r_{1M} r_{M2} \exp(2i\beta_M d)}, \quad (1)$$

where $\beta_M = \sqrt{\varepsilon_M \mu_M \varepsilon_0 \mu_0 (\omega/c)^2 - k_x^2}$, and t and r are Fresnel coefficients of transmission and reflection at interfaces indicated by subscripts. Please note that for a perfect imaging system, the OTF should remain constant regardless of the variation of k_x .

In order to find the imaging properties, we decomposed the incident object field \mathbf{H}_{obj} at $(-u < z < 0)$ impressed by the object into superposition of lateral components with the help of the Weyl integral:

$$\mathbf{H}_{\text{obj}}(x, -u < z < 0) = \frac{\nabla \times \hat{z}}{4\pi} \int_{-\infty}^{\infty} dk_x \frac{\exp(ik_x x + i\beta_1 |z+u|)}{i\beta_1} I(k_x, \beta_1), \quad (2)$$

where $I(k_x, \beta_1)$ represents the Fourier transform of line current source $I\delta(\mathbf{r}-\mathbf{r}')$.

As a result, the image field at focal point $z=d+v$ is simply the convolution of the source field and the OTF:

$$\mathbf{H}_{\text{img}}(x, z=d+v) = \frac{\nabla \times \hat{z}}{4\pi} \int_{-\infty}^{\infty} dk_x \frac{\exp(ik_x x)}{i\beta_1} I(k_x) \text{OTF}(k_x). \quad (3)$$

A key function of the metalens is to transmit the lateral field component of an object at a large spatial frequency k_x with enhanced amplitude. In symmetrical case ($\varepsilon_1 = \varepsilon_2 = 1$ and $\mu_1 = \mu_2 = 1$), the TM transmission coefficient T_P reads:

$$T_P = \frac{4\varepsilon_M \beta_1 \beta_M}{(\varepsilon_M \beta_1 + \beta_M)^2 \exp(-i\beta_M d) - (\varepsilon_M \beta_1 - \beta_M)^2 \exp(i\beta_M d)}. \quad (4)$$

It can be further simplified to

$$T_P = 2\varepsilon_M \beta_1 (1/L^+ - 1/L^-), \quad (5)$$

where $L^+ = \varepsilon_M \beta_1 + \beta_M \tanh(-i\beta_M d/2)$ (Ref. 7) and $L^- = \varepsilon_M \beta_1 + \beta_M \coth(-i\beta_M d/2)$. Thus, for large k_x and $\varepsilon_M \neq -1$, the off-resonance transmission reads:

$$T_P \approx 8\varepsilon_M (\varepsilon_M + 1)^{-2} \exp(-|k_x|d). \quad (6)$$

It can be seen from Eq. (6) that T_P decays exponentially with the increasing thickness d . Thus, for a large mismatch ($|\delta\varepsilon| > 1$), the resolution limit as a rule of thumb is $\sim 2d$. Alternately, when the surface resonance occurs (L^+ or $L^- \rightarrow 0$), the transmission is at a local maximum. Therefore, the field components near the resonance are disproportionately enhanced in the resulting image.^{8,9}

Although LHM's are realized in the microwave range,^{2,3,10} essential engineering methods have to be developed in order to meet the critical demand of desired values of ε and μ toward a functional superlens. As an initial effort, we focused on the negative ε properties since this is the only relevant material response to TM light in the electrostatic limit. To illustrate the sensitivity of image resolution dependence on the material properties mismatch, we plot the modulation transfer function ($\text{MTF} = |\text{OTF}|^2$) of a metalens due to mismatch of ε in Fig. 2. It is clear that in order to achieve a high spatial resolution ($< \lambda/10$) in a metalens, the

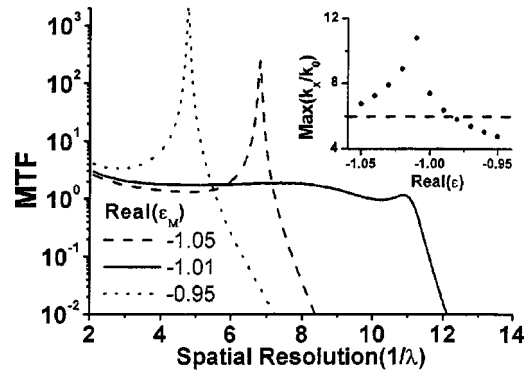


FIG. 2. The MTF of a LHM superlens exhibits lower cutoff due to mismatch of ε . The thickness d of the lens is $\lambda/10$, with $\mu = 1$, $\text{Imag}(\varepsilon_M) = 0.001$. The inset depicts the displacement of surface resonance peak as a function of mismatch of ε .

variance of ε_M should be better than 1%. Interestingly, the cutoff of a spatial resolution always follows the resonant peak due to the excitation of surface waves. As a practical rule, we can locate these peaks as a guideline of the cutoff of the spatial frequency. In the quasistatic limit, the peaks can be predicted by $\max(k_x/k_0) = \lambda \log(2/|\delta\varepsilon|)/2\pi d$. This is in good agreement with our simulation, as shown in the inset of

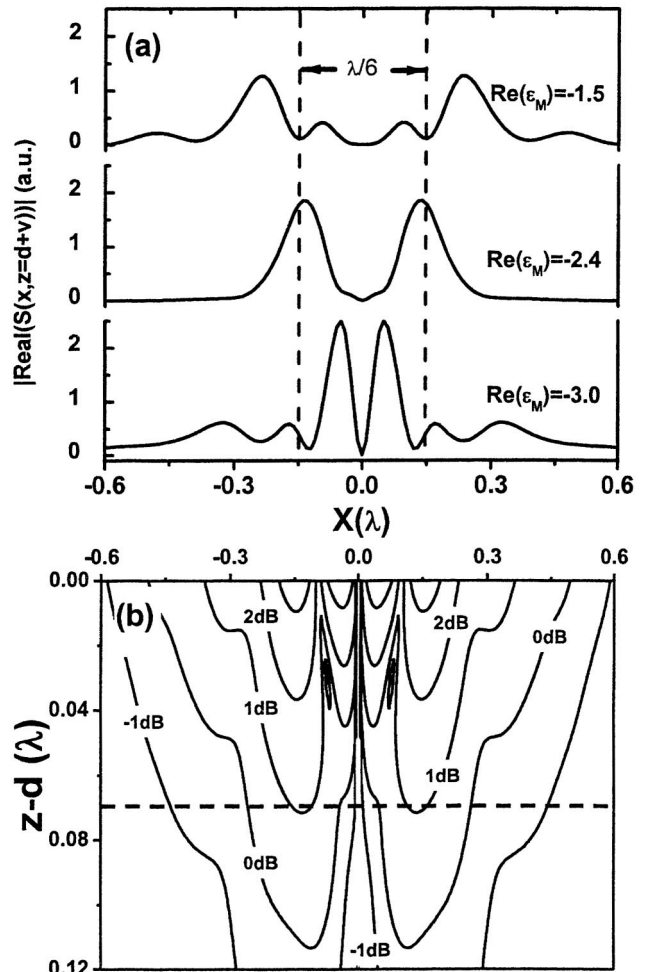


FIG. 3. (a) The image collected at the paraxial focal plane with the original sources separated by $\lambda/6$; Panel (b) shows the logarithmic contour of power density $|\text{Real}(S(x, z))|$ in medium 2 for the case of $2a = \lambda/6$, $\varepsilon_M = -2.4 + i0.27$, $\varepsilon_1 = 2.368$, and $\varepsilon_2 = 2.79$. The dashed line in (b) corresponds to the paraxial focal plane.

Fig. 2. Furthermore, it turns out that the effect of loss characterized by the imaginary part of ϵ can also be approximated in this equation.¹¹ In the case of $\text{Imag}(\epsilon_M) = 0.4$, the result is approximately 2.6, indicating a resolution of $\sim \lambda/3$. Taking the loss of natural metal at optical frequencies into account, the constraints of near-field imaging still exist at the current stage in order to achieve subwavelength resolution,^{12,13} yet the metalens does indeed offer significantly improved contrast. In concert with future physical discoveries of metamaterials, applications of the metalens to far-field imaging will come true.

It is clear from this discussion that to further improve the resolution limit in the superlens, we must consider a surrounding medium with dielectric function $\epsilon > 1$. For instance, we select medium 1 to be glass ($\epsilon_1 = 2.368$), and medium 2 to be a photoresist ($\epsilon_2 = 2.79$). In this case, we are facing a slightly asymmetric condition, with $\text{Imag}(\epsilon_M) = 0.27$. The simulation result of average Poynting vector $|\text{Real}(\mathbf{S}(x, z))|$ at the paraxial focal plane, $z = d + v$, is shown in Fig. 3(a). It can be found that a resolution of $\lambda/6$ is achieved at $\text{Real}(\epsilon_M) = -2.4$, which corresponds to 364 nm wavelength. In addition, when ϵ_M is tuned to increasingly negative values, we obtain a compressed image [$\text{Real}(\epsilon_M) = -3.0$ case in Fig. 3(a)]. In contrast, an expanded image is observable at a less negative ϵ_M . Unlike the magnification or demagnification in conventional optics, these phenomena should be attributed to the contribution of surface resonances which detuned the lateral peak width¹² and position. This argument can be justified by the adjacent harmonic peaks in the case of $\text{Real}(\epsilon_M) = -1.5$ and -3.0 .

Finally, to record this near-field image, we can now consider a nearly loss-free photoresist as medium ϵ_2 , which is only sensitive to the power density distribution. In this case, we select $\epsilon_M = -2.4$, while the other conditions remain unaltered as in Fig. 3(a). The simulation result is shown in Fig. 3(b). Counterintuitively, we do not observe the highest power flux at focal points in the case of superlens imaging, in contrast to the conventional imaging situation. The origin of this

effect is related to the decaying nature of the evanescent field. In order to restore the strength of the evanescent field at the image plane, the field strength is indeed much higher on the surface of the superlens. The elevated evanescent field strength at the exit of the superlens outweighs the contribution from propagating waves, so that the phase contour⁸ or the streamline of Poynting vector¹² instead of the power flux should be chosen as a measure in determination of the focal plane. On the other hand, the “paraxial” image plane at $v = |n_2/n_M|d - |n_M/n_1|u$ is still helpful as it offers the optimal intensity contrast of the transferred image,¹³ although the definition of the depth of an image field remains to be re-examined in the case of the superlens.

The authors are grateful to Dr. S. A. Ramakrishna and Professor J. B. Pendry of Imperial College and Professor D. Smith of UCSD for helpful discussions. This work is supported by the MURI (Grant No. N00014-01-1-0803), ONR (Grant No. N00014-02-1-0224), and the NSF (Grant No. DMI-9703426).

- ¹H. Kosaka, T. Kawashima, A. Tomita, M. Notomi, T. Tamamura, T. Sato, and S. Kawakami, *Phys. Rev. B* **58**, R10096 (1998).
- ²D. R. Smith, W. Padilla, D. C. Vier, S. C. Nemat-Nasser, and S. Schultz, *Phys. Rev. Lett.* **84**, 4184 (2000).
- ³R. Shelby, D. R. Smith, and S. Schultz, *Science* **292**, 77 (2001).
- ⁴V. G. Veselago, *Sov. Phys. Usp.* **10**, 509 (1968).
- ⁵J. B. Pendry, *Phys. Rev. Lett.* **85**, 3966 (2000).
- ⁶M. Notomi, *Phys. Rev. B* **62**, R10696 (2000).
- ⁷H. Raether, *Excitation of Plasmons and Interband Transitions by Electrons* (Springer, Berlin, 1980), Chap. 10.
- ⁸R. W. Ziolkowski and E. Heyman, *Phys. Rev. E* **64**, R056625 (2001).
- ⁹S. A. Ramakrishna, J. B. Pendry, D. Schurig, D. R. Smith, and S. Schultz, *J. Mod. Opt.* **49**, 1747 (2002).
- ¹⁰T. Weiland, R. Schuhmann, R. B. Greegor, C. G. Parazzoli, A. M. Vetter, D. R. Smith, D. C. Vier, and S. Schultz, *J. Appl. Phys.* **90**, 5419 (2001).
- ¹¹S. A. Ramakrishna, J. B. Pendry, M. C. K. Wiltshire, and W. J. Stewart, *J. Mod. Opt.* (to be published).
- ¹²E. Shamonina, V. A. Kalinin, K. H. Ringhofer, and L. Solymar, *Electron. Lett.* **37**, 1243 (2001).
- ¹³For example, see J. T. Shen and P. M. Platzman, *Appl. Phys. Lett.* **80**, 3286 (2002); where a $\epsilon_M = -1$ imaging case is given by considering retardation.